

ChemComm

Accepted Manuscript



This article can be cited before page numbers have been issued, to do this please use: Y. Yoon, S. Jo, S. J. Park, H. M. Kim, D. Kim and T. S. Lee, *Chem. Commun.*, 2019, DOI: 10.1039/C9CC03106E.



This is an Accepted Manuscript, which has been through the Royal Society of Chemistry peer review process and has been accepted for publication.

Accepted Manuscripts are published online shortly after acceptance, before technical editing, formatting and proof reading. Using this free service, authors can make their results available to the community, in citable form, before we publish the edited article. We will replace this Accepted Manuscript with the edited and formatted Advance Article as soon as it is available.

You can find more information about Accepted Manuscripts in the [author guidelines](#).

Please note that technical editing may introduce minor changes to the text and/or graphics, which may alter content. The journal's standard [Terms & Conditions](#) and the ethical guidelines, outlined in our [author and reviewer resource centre](#), still apply. In no event shall the Royal Society of Chemistry be held responsible for any errors or omissions in this Accepted Manuscript or any consequences arising from the use of any information it contains.

COMMUNICATION

Unusual fluorescence of *o*-phenylazonaphthol derivatives with aggregation-induced emission and their use in two-photon cell imagingReceived 00th January 20xx,
Accepted 00th January 20xx

DOI: 10.1039/x0xx00000x

Yeoju Yoon,^a Seonyoung Jo,^a Sang Jun Park,^b Hwan Myung Kim,^b Dongwook Kim,^c and Taek Seung Lee^{*a}

o-Phenylazonaphthol (*o*-PAN) derivatives including 6-bromo-1-((4-bromophenyl)diazanyl) naphthalen-2-ol (AN-Br-OH) and 1-phenylazo-2-naphthol (AN-OH, known as Sudan I (Color Index 12055)) were synthesized to investigate their fluorogenic behaviors, in which their aggregated-induced emission (AIE) is reported. The *o*-PANs showed a two-photon absorption. The protection of hydroxyl groups in *o*-PANs was used for fluorescent imaging of esterase-expressed HepG2 cells, which is potentially suitable for sensing and two-photon cell imaging applications.

Azobenzenes have been used as reversible photochromic materials because of their *trans-cis* photoisomerization.^{1,2} The photoisomerization of azobenzene has been used in various fields such as optical information storage,³ light-triggered switching,⁴ and reversible and storage devices.⁵ Azobenzenes have been known as nonfluorescent species, because: i) the nonbonding electrons in the nitrogen quench the fluorescence; and ii) they undergo a process of efficient photoisomerization in the photoexcited state.^{6,7} Several studies on the fluorescence of azobenzene derivatives have been reported, but most of them require complicated chemical structures or self-assembly of azobenzene to obtain the fluorescent azobenzenes.⁸⁻¹⁰

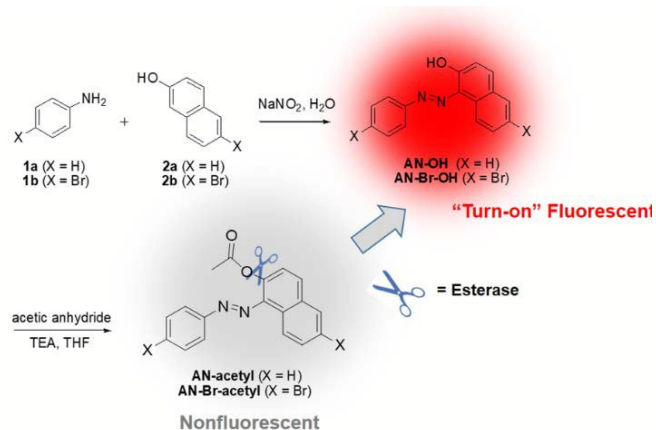
Organic fluorescent materials have attracted much interest because of their easy synthesis and low cost compared with inorganic materials. However, most organic fluorescent materials rarely fluoresce in their solid states, an effect known as aggregation-caused quenching (ACQ). The inverse phenomenon of ACQ, known as AIE was discovered.^{11,12} The AIE-active luminogens are weak or nonemissive in solution; however, their fluorescence increases in the solid or aggregated state.¹³⁻¹⁵ The AIE-active luminogens have been applied in many fields such as biosensors,¹⁶⁻¹⁸ optoelectronic devices,^{19,20} chemical probes.²¹ As the azobenzenes do not exhibit effective

fluorescence, they intrinsically do not provide AIE. An AIE-active azobenzene was reported via self-assembly of azobenzene to form nanofibers.²²

A number of small molecular probes have been used to detect a variety of biological targets.²³ Among such targets, the detection of esterase activity has gained much interest because this activity is directly related to human diseases such as obesity, cancer, hyperlipidemia, and hepatic steatosis.²⁴⁻²⁵ One of the versatile detection methods of esterase is based on enzymatic hydrolysis of the functional groups in the probes. For example, the ester-protected hydroxyl group is converted to the hydroxyl group by esterase-induced enzymatic hydrolysis, leading to modulation of the fluorescence signal.^{26,27}

Herein, we are reporting for the first time on an unusual fluorescence from *o*-PANs; moreover, a higher fluorescence intensity was observed in their solid states, known as AIE. The AIE was caused by the unique structure of *o*-PANs, which have intramolecular hydrogen bonding induced by the hydroxyl groups of the *o*-PANs. Subsequent two-photon esterase sensing and imaging were investigated using protection and deprotection of the hydroxyl group, providing a "turn-on" fluorescent sensor. We propose the *o*-PANs as potential candidates for esterase detection and two-photon imaging.

o-PAN-based compounds such as AN-OH and AN-Br-OH were synthesized via diazotization and an azo-coupling reaction



Scheme 1. Synthetic route to *o*-PAN derivatives and schematic illustration of "turn-on" fluorescent probes for esterase.

^a Organic and Optoelectronic Materials Laboratory, Department of Advanced Organic Materials and Textile System Engineering, Chungnam National University Daejeon 34134, Korea. E-mail: tslee@cnu.ac.kr

^b Department of Chemistry and Department of Energy Systems Research, Ajou University, Suwon 16499, Korea

^c Department of Chemistry, Kyonggi University, Suwon 16227, Korea

† Footnotes relating to the title and/or authors should appear here.

Electronic Supplementary Information (ESI) available: [Experimental details; tautomeric structures; fluorescence of Azo-acetate and Azo-Br-acetate; fluorescence in PMMA film; DFT; TP spectrum]. See DOI: 10.1039/x0xx00000x

between corresponding aromatic amines and naphthols (Scheme 1).²⁸ AN-OH was synthesized from aniline and 2-naphthol and AN-Br-OH was obtained from p-bromoaniline and 6-bromo-2-naphthol. For further application to esterase sensing, the hydroxyl groups of AN-OH and AN-Br-OH were protected with acetyl groups to synthesize AN-acetate and AN-Br-acetate. The UV absorption of AN-OH and AN-Br-OH are shown at 487 and 482 nm, respectively, exhibiting red color (Fig. S1a). After conversion of the hydroxyl group to the acetate group, absorption of AN-acetate and AN-Br-acetate was blue-shifted to 360 and 370 nm, respectively, indicating that the intramolecular hydrogen bond was the main cause of the red color of the molecules. Unlike most nonfluorescent azobenzene compounds, the fluorescence emission of AN-OH and AN-Br-OH in their solid states was observed at 602 (reddish orange) and 630 nm (red), respectively, whereas their acetylated compounds (AN-acetate and AN-Br-acetate) were nonfluorescent in their solid states. Neither AN-acetate nor AN-Br-acetate exhibited significant fluorescence in their solid or in the solution states (Fig. S1b,c), mainly because of the absence of the hydroxyl groups. The hydroxyl groups in AN-OH and AN-Br-OH were necessary to provide the red color and fluorescence. Such a chromogenic behavior of o-PAN derivatives was already elucidated by the protection and deprotection of the hydroxyl groups,^{28,29} whereas their fluorogenic behavior has never been investigated.

Unexpectedly, AIE was observed in the solid states of AN-OH and AN-Br-OH, not in their solutions. To confirm the AIE of the compounds, we investigated the effects of the concentrations of AN-OH and AN-Br-OH on their fluorescence in THF. The AIE property was investigated by measuring the changes in the fluorescence in various water volume fractions ($f_w = 0\sim 90\%$) in THF solution. The red fluorescence of AN-Br-OH at 625 nm increased with increasing the water fraction, resulting from the aggregation of AN-Br-OH (Fig. 1a,b). The aggregation of AN-OH induced an abrupt generation of orange emission from the 60% water volume fraction (Fig. 1c,d). The AIE of the compounds could be clearly seen by the naked eye (inset photographs of Fig. 1b,d). o-PANs did not show fluorescence in other solvents such as acetone, chloroform, and DMF. The AIE characteristics were also confirmed in their solid solutions. Spin-cast thin films of poly(methyl methacrylate) (PMMA) containing various amounts of o-PANs, and the changes in the films' fluorescence were investigated (Fig. S2). The PMMA films containing AN-Br-OH and AN-OH displayed red emission at 614 and at 612 nm, respectively, and the emission intensity increased as the concentration of these compounds increased. Like the experiment performed in the solution, noticeable AIE was also observed in their solid solutions. The fluorescence wavelength of the o-PAN compounds in PMMA was red-shifted from 590 to about 610 nm with an increase in their concentrations, suggesting intensified intermolecular interaction between the PMMA and the o-PAN compounds. The fluorescence QYs of AN-Br-OH and AN-OH were found to be 0.012 and 0.014, respectively. Although they showed low values, but higher than that previously reported azobenzene (0.008).²²

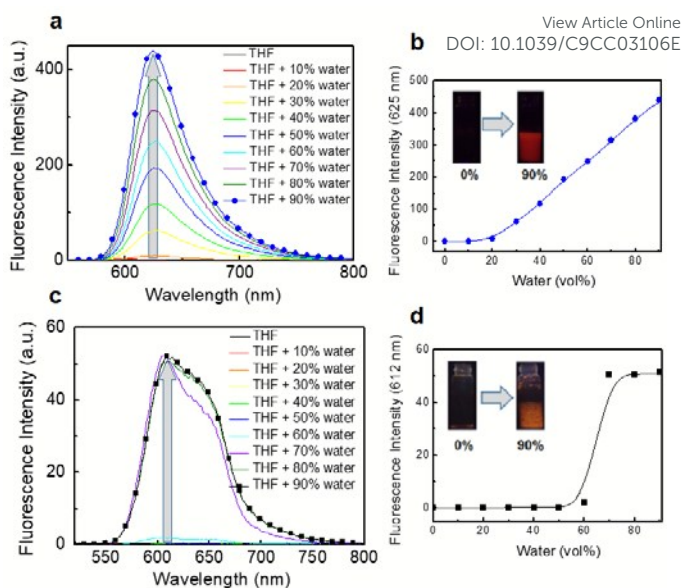


Fig. 1. Changes in the fluorescence spectra of (a) AN-Br-OH (2.5×10^{-2} M) and (c) AN-OH (8.06×10^{-2} M) in the presence of water (0 to 90 vol%). Plots of the fluorescence intensity of (b) AN-Br-OH and (d) AN-OH versus water fraction in THF/water mixture. Inset photographs represent AN-Br-OH and AN-OH in THF in the presence of water under UV light (365 nm).

It was already reported that AN-OH had intermolecular hydrogen bonding and secondary interactions including π - π stacking and charge-dipole interaction to provide the stable monoclinic crystalline structure of AN-OH.³⁰ The monoclinic crystal system of AN-OH provides the planarity of the molecule. We investigated the XRD pattern of AN-Br-OH and analyzed the crystal system, indicating the monoclinic crystalline structure of AN-Br-OH, similar to AN-OH (Table S1). It was expected that the AIE from AN-Br-OH and AN-OH was caused by identical factors, i.e., the strong intramolecular hydrogen bond and the intermolecular π - π interactions provided restrictions for intramolecular rotation and dense packing, thus activating the radiation pathway.^{31,32} The hydroxyl groups in AN-Br-OH and AN-OH induced the intramolecular hydrogen bonding, resulting in the planarization of the molecules (Scheme S1). The o-PAN derivatives have a strong intramolecular hydrogen bonding induced by azo-hydrazo tautomerism. As a result, the intramolecular rotation was restricted in the hydrazo tautomer and this, in turn, contributed to the fluorescence enhancement in the solid state. The DFT calculation of AN-OH and AN-Br-OH was performed to determine the HOMO and the LUMO band levels using the B3LYP/6-31G(d) set (Fig. S3). The energy band gap of AN-Br-OH (3.32 eV) is smaller than that of AN-OH (3.42 eV), presumably because of the electron-withdrawing bromo groups. The electrons in the LUMO state of AN-Br-OH are more delocalized than AN-OH, resulting in a smaller band gap of AN-Br-OH.

As esterase is an enzyme that can effectively cleave an ester linkage in a molecule, AN-acetate and AN-Br-acetate could be used as esterase probes (Scheme 1). The probes were virtually nonfluorescent both in solution and in the solid state. The acetate groups both in AN-acetate and AN-Br-acetate could be easily cleaved by esterase and transformed into hydroxyl

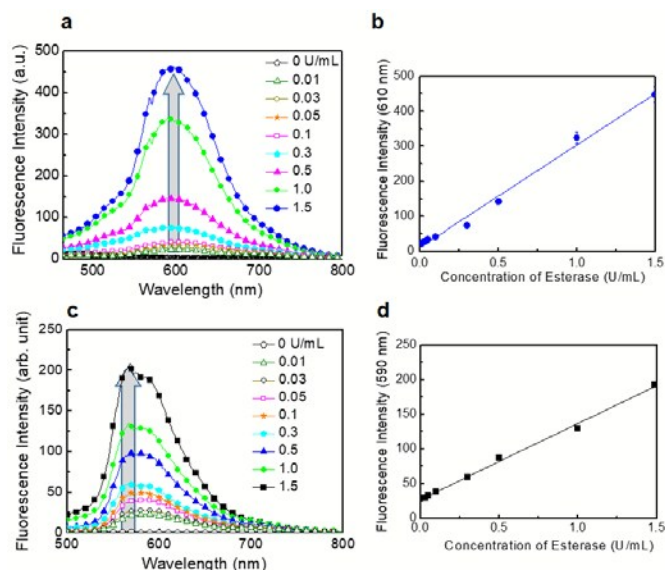


Fig. 2. Changes in fluorescence spectra of (a) AN-Br-acetate and (c) AN-acetate with various esterase concentrations (incubation time: 30 min). Relationship between the fluorescence intensity and the esterase concentrations of (b) AN-Br-acetate and (d) AN-acetate in the range of 0 - 0.15 U/mL.

groups, resulting in the recovery of red fluorescent AN-OH and AN-Br-OH. The fluorescence intensity of AN-acetate and AN-Br-acetate increased with increasing incubation time with esterase (0.10 U/mL) and saturated at 12 min and 30 min, respectively, indicating that a faster enzymatic hydrolysis was performed using AN-acetate (Fig. S4). New fluorescence emission bands were observed at 610 (AN-Br-OH) and 590 nm (AN-OH), which corresponded to emission bands of the respective compounds. This indicates that enzymatic hydrolysis of ester groups took place to form hydroxyl groups, inducing “turn-on” fluorescence. The inset photographs indicate that the changes in the color and fluorescence color of the probes enabled us to monitor the esterase activity by the naked eye.

To determine the limits of detection (LODs), the changes in the fluorescence spectra of AN-Br-acetate and AN-acetate were investigated at various esterase concentrations (0 to 1.5 U/mL) (Fig. 2). The LODs were calculated to be 1.87×10^{-3} U/mL (R^2 : 0.99261) and 2.75×10^{-3} U/mL (R^2 : 0.9893) for AN-Br-acetate and AN-acetate, respectively, based on the $3\sigma/\text{slope}$, where σ is the standard deviation of four independent measurements. The LODs were higher than the results obtained in previous studies.^{26,27} Selectivity is an important factor in assessing the probes for biological applications. Other enzymes including glucose oxidase (GOx), trypsin, and pepsin were used to investigate the selective detection of esterase (Fig. 3a,b). Upon exposure of the probes to enzymes, only esterase led to remarkable fluorescence changes, indicating that selective hydrolysis took place in the presence of esterase.

To elucidate the enzymatic hydrolytic efficiency of AN-Br-acetate and AN-acetate, the kinetic parameters (k_{cat}/K_m) of the enzymatic hydrolysis of the probes were determined by Lineweaver-Burk analysis (Fig. S5). The k_{cat} is a rate constant of in which a large k_{cat} indicates a fast reaction. K_m is an equilibrium constant for the binding of probes to an enzyme, in which a

small K_m represents tight binding to the enzyme. The AN-Br-acetate showed a better affinity for the esterase than AN-acetate, judging from the k_{cat}/K_m values ($218 \text{ M}^{-1}\text{sec}^{-1}$ and $29 \text{ M}^{-1}\text{sec}^{-1}$, respectively). The two probes can be used in biological systems for esterase detection.

We found that AN-Br-OH and AN-OH had TP activity, in which the most feasible excitation was observed at 900 nm (Fig. S6). The two compounds could be excited at 900 nm (corresponding to the near infrared region) to emit red fluorescence, and thus enabled it to prevent autofluorescence and cell damage that were usually encountered when using one-photon microscopy (OPM).³² It has been reported that most fluorescent probes used in TPM were virtual OP probes and not suitable for TPM, and thus they had low TPA cross-sections of less than 50 in Göppert-Mayer units (δ).³³ The TPA cross-section values of AN-OH and AN-Br-OH at 900 nm were found to be 81 and 73 GM, respectively. Because such high δ values indicated a high TP absorption efficiency, AN-Br-acetate and AN-acetate could be applicable to TP bioimaging. The TP absorptivity resulted from planarization of the geometry upon aggregation, leading to packing in the aggregated state.³⁴

To evaluate the biological safety of the probes, their cell viability was investigated using HeLa cells measured by an MTT assay (Fig. S7). Cell viability was not significantly affected by the cell concentration and incubation time of AN-acetate. Regarding AN-Br-acetate, it did not show effective biocompatibility. Therefore, it was found that the cytotoxicity of AN-acetate was lower than that of AN-Br-acetate, suggesting that the former was more suitable for cell imaging. It seems that the lower cell viability of AN-Br-acetate probes resulted from the halogen groups in the molecule. The cell uptake of AN-Br-acetate and AN-acetate was carried out by incubation of cells with the two probes. HepG2 cells were used, because esterase was overexpressed in the cells.²⁷

The HepG2 cells were incubated with AN-Br-acetate and AN-acetate for 30 min. After the incubation, a stronger fluorescence was observed in the HepG2 cells. It indicated that free hydroxyl groups were formed by enzymatic hydrolysis of AN-Br-acetate and AN-acetate probes, which were converted to AN-Br-OH and AN-OH, respectively (Fig. 4 and S8). The cell imaging in HepG2 cells was successfully accomplished by TP as well as one-photon (OP) excitation. For the inhibitor test,

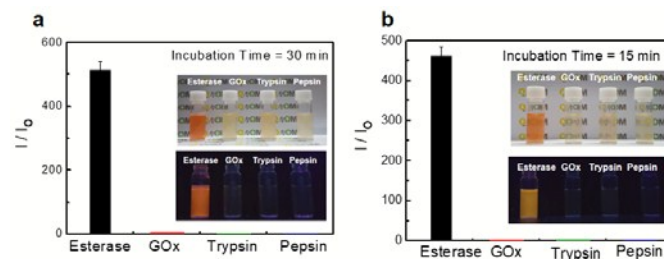


Fig. 3. Changes in the fluorescence of (a) AN-Br-acetate and (b) AN-acetate (10 mM) upon exposure to other enzymes (0.1 U/mL) in 10 mM PBS buffer solution at pH 7.2, 37°C. Inset photographs were taken in the presence of enzymes under ambient light (upper) and UV light (365 nm). I_0 and I correspond to fluorescence intensity of (a) AN-Br-acetate (606 nm) and (b) AN-acetate (580 nm) before and after incubation with enzymes, respectively.

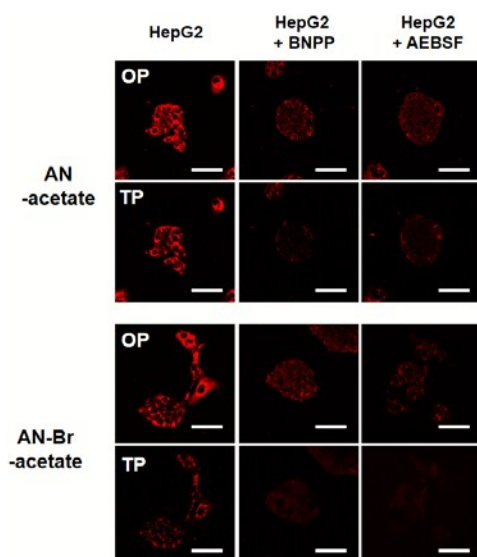


Fig. 4. OPM and TPM images of HepG2 cells incubated with AN-acetate (10 μ M) and AN-Br-acetate (10 μ M) for 30 min. For the inhibition test, HepG2 cells were pretreated with BNPP (500 μ M) and AEBSF (2 mM) for 30 min and then incubated with the probes. Scale bars = 50 μ m.

HepG2 cells were pretreated with bis(4-nitrophenyl) phosphate (BNPP) and 4-(2-aminoethyl)benzenesulfonyl fluoride hydrochloride (AEBSF) for 30 min and were then incubated with the probes, in which BNPP and AEBSF inhibited the enzymatic hydrolysis by esterase. The HepG2 cells pretreated with BNPP and AEBSF showed a lower fluorescence intensity than untreated HepG2 cells. To check the photostability of the probes, the fluorescence intensity of the probes was investigated according to imaging time (Fig. S9). The photostability of probes in cells was investigated by continuous exposure to laser sources with 488 (for OP) and 900 nm (for TP). The fluorescence intensity of both probes did not significantly change in HepG2 cells after 60 min irradiation, demonstrating the high photostability of the probes. The small increase in the fluorescence using OP was presumed to result from the autofluorescence.

In summary, we demonstrated the unusual fluorescence generated by AIE-active o-PAN luminogens. The o-PANs had a TPA property, enabling long wavelength (900 nm) excitation, which would be beneficial for biological cell imaging. The AN-Br-acetate and AN-acetate probes showed high selectivity and sensitivity toward esterase, by which they can be considered as potential candidates for esterase enzyme detection and TP cell imaging. This work was supported by the National Research Foundation (NRF) of Korean government through Basic Science Research Program (2018R1A2A2A14022019).

Conflicts of interest

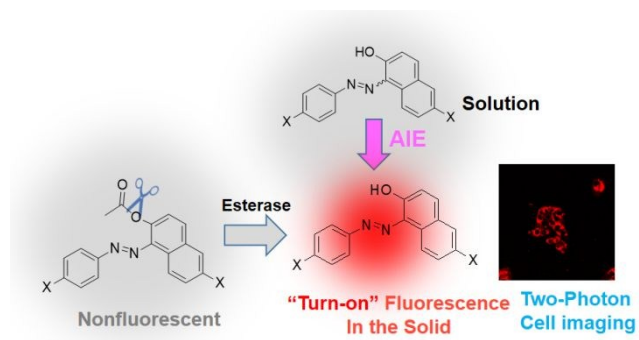
There are no conflicts to declare.

Notes and references

- 1 A. A. Beharry, G. A. Woolley, *Chem. Soc. Rev.* 2011, **40**, 4422.
- 2 W. Szymanski, J. M. Beierle, H. A. V. Kistemaker, W. A. Velema, B. L. Feringa, *Chem. Rev.* 2013, **113**, 6114.

- 3 A. R. Yuvaraj, S. Kumar, *Gen. Chem.* 2018, **4**, 170020.
- 4 G. Markiewicz, D. Pakulski, A. Galanti, V. Patroniak, A. Ciesielski, A. R. Stefankiewicz, P. Samorì, *Chem. Commun.* 2017, **53**, 7278.
- 5 S. Li, G. Han, W. Zhang, *Macromolecules* 2018, **51**, 4290.
- 6 J. Yoshino, N. Kano, T. Kawashima, *Chem. Commun.* 2007, **14**, 559.
- 7 W. Piao, S. Tsuda, Y. Tanaka, S. Maeda, F. Liu, S. Takahashi, Y. Kushida, T. Komatsu, T. Ueno, T. Terai, T. Nakazawa, M. Uchiyama, K. Morokuma, T. Nagano, K. Hanaoka, *Angew. Chem. Int. Ed.* 2013, **52**, 13028.
- 8 M. Han, M. Hara, *J. Am. Chem. Soc.* 2005, **127**, 10951.
- 9 X. Ran, H. Wang, L. Shi, J. Lou, B. Liu, M. Li, L. Guo, *J. Mater. Chem. C* 2014, **2**, 9866.
- 10 J. Yoshino, N. Kano, T. Kawashima, *Dalton Trans.* 2013, **42**, 15826.
- 11 J. Qian, B. Z. Tang, *Chem.* 2017, **3**, 56.
- 12 H. Wang, E. Zhao, J. W. Y. Lam, B. Z. Tang, *Mater. Today* 2015, **18**, 365.
- 13 V. S. Padalkar, K. Kuwada, D. Sakamaki, N. Tohnai, T. Akutagawa, K. Sakai, T. Sakurai, S. Seki, *ChemistrySelect* 2017, **2**, 1959.
- 14 H. Naito, K. Nishino, Y. Morisaki, K. Tanaka, Y. Chujo, *Angew. Chem. Int. Ed.* 2017, **56**, 254.
- 15 B. Liu, H. Nie, G. Lin, S. Hu, D. Gao, J. Zou, M. Xu, L. Wang, Z. Zhao, H. Ning, J. Peng, Y. Cao, B. Z. Tang, *ACS Appl. Mater. Interfaces* 2017, **9**, 34162.
- 16 J. Mei, Y. Huang, H. Tian, *ACS Appl. Mater. Interfaces* 2018, **10**, 12217.
- 17 X. He, Z. Zhao, L. Xiong, P. F. Gao, C. Peng, R. S. Li, Y. Xiong, Z. Li, H. H. Y. Sung, I. D. Williams, R. T. K. Kwok, J. W. Y. Lam, C. Z. Huang, N. Ma, B. Z. Tang, *J. Am. Chem. Soc.* 2018, **140**, 6904.
- 18 Z. Song, R. T. K. Kwok, E. Zhao, Z. He, Y. Hong, J. W. Y. Lam, B. Liu, B. Z. Tang, *ACS Appl. Mater. Interfaces* 2014, **6**, 17245.
- 19 L. Yao, S. Zhang, R. Wang, W. Li, F. Shen, B. Yang, Y. Ma, *Angew. Chem. Int. Ed.* 2014, **53**, 2119.
- 20 J. A. H. P. Sol, V. Dehm, R. Hecht, F. Würthner, A. P. H. Schenning, M. G. Debije, *Angew. Chem. Int. Ed.* 2018, **57**, 1030.
- 21 Q. Hu, M. Gao, G. Feng, X. Chen, B. Liu, *ACS Appl. Mater. Interfaces* 2015, **7**, 4882.
- 22 H. Han, S. J. Cho, Y. Norikane, M. Shimizu, A. Kimura, T. Tamagawa, T. Seki, *Chem. Commun.* 2014, **50**, 15815.
- 23 a) Q. Xu, T. Kuang, Y. Liu, L. Cai, X. Peng, T. S. Sreeprasad, P. Zhao, Z. Yu and N. Li, *J. Mater. Chem. B* 2016, **4**, 7204; b) P. Miao, B. Wang, Z. Yu, J. Zhao and Y. Tang, *Biosens. Bioelectron.* 2015, **63**, 365; c) Y. Cui, B. Li, H. He, W. Zhou, B. Chen and G. Qian, *Acc. Chem. Res.* 2016, **49**, 483–493; d) D. Kim, J. Kim and T. S. Lee, *Sens. Actuat. B: Chem.* 2018, **264**, 45.
- 24 a) M. Tian, J. Sun, Y. Tang, B. Dong, W. Lin, *Anal. Chem.* 2018, **90**, 998; b) F. Derikvand, D. T. Yin, R. Barrett, H. Brumer, *Anal. Chem.* 2016, **88**, 2989.
- 25 S. J. Park, H. W. Lee, H. Kim, C. Kang, H. M. Kim, *Chem. Sci.* 2016, **7**, 3703.
- 26 L. Peng, S. Xu, X. Zheng, X. Cheng, R. Zhang, J. Liu, B. Liu, A. Tong, *Anal. Chem.* 2017, **89**, 3162.
- 27 S. Kim, H. Kim, Y. Choi, Y. Kim, *Chem. Eur. J.* 2015, **21**, 9645.
- 28 M. S. Choi, J. H. Lee, D. W. Kim, T. S. Lee, *J. Polym. Sci., Part A: Polym. Chem.* 2007, **45**, 4430.
- 29 C. Kocher, C. Weder, P. Smith, *Adv. Funct. Mater.* 2003, **13**, 427.
- 30 G. R. Ferreira, H. C. Garcia, M. R. C. Couri, H. F. D. Santos, L. F. C. Oliveira, *J. Phys. Chem. A* 2013, **117**, 642.
- 31 X. Ma, R. Sun, J. Cheng, J. Liu, F. Gou, H. Xiang, X. Zhou, *J. Chem. Educ.* 2016, **93**, 345.
- 32 a) B. Li, T. He, X. Shen, D. Tang, S. Yin, *Polym. Chem.* 2019, **10**, 796; b) H. Chen, Y. Tang, H. Shang, X. Kong, R. Guo, W. Lin, *J. Mater. Chem. B* 2017, **5**, 2436.
- 33 H. M. Kim, B. R. Cho, *Chem. Rev.* 2015, **115**, 5014.
- 34 S. Kim, T. Y. Ohulchanskyy, H. E. Pudavar, R. K. Pandey and P. N. Prasad, *J. Am. Chem. Soc.* 2007, **129**, 2669.

Table of Contents



Unusual fluorescence of *o*-phenylazonaphthol derivatives with aggregated-induced emission (AIE) is reported for the first time, which can be used in two-photon cell imaging applications